

Inclusive h_c production at B factories

Yu Jia^{*,1,2} Wen-Long Sang^{†,1,2} and Jia Xu^{‡1}

¹*Institute of High Energy Physics, Chinese Academy of Sciences, Beijing 100049, China*

²*Theoretical Physics Center for Science Facilities,
Chinese Academy of Sciences, Beijing 100049, China*

(Dated: September 16, 2018)

Abstract

Within the nonrelativistic QCD (NRQCD) factorization framework, we investigate the inclusive production of the h_c meson associated with either light hadrons or charmed hadrons at B factory energy $\sqrt{s} = 10.58$ GeV. Both the leading color-singlet and color-octet channels are included. For the h_c production associated with light hadrons, the total production rate is dominated by the color-octet channel, thus the future measurement of this process may impose useful constraint on the value of the color-octet matrix element $\langle \mathcal{O}_8^{h_c}(^1S_0) \rangle$; for the h_c production associated with charmed hadrons, the total production rate is about one order of magnitude smaller, and dominated by the color-singlet channel.

PACS numbers: *12.38.-t, 12.39.St, 13.60.Hb, 14.40.Pq*

* jia@ihep.ac.cn

† swlong@itp.ac.cn

‡ xuj@ihep.ac.cn

I. INTRODUCTION

The lowest-lying $c\bar{c}(^1P_1)$ state, the $h_c(1P)$ meson, is the last one found among all the charmonium members below open charm threshold. This elusive particle was not firmly established until 2005, through the isospin-violating decay $\psi' \rightarrow \pi^0(\rightarrow \gamma\gamma)h_c(\rightarrow \eta_c\gamma)$ by CLEO Collaboration [1], as well as through the process $p\bar{p} \rightarrow h_c \rightarrow \eta_c\gamma$ by the E835 experiment [2]. Quite recently, the analogous 1P_1 members in the bottomonium family, the $h_b(1P, 2P)$ mesons, have also been observed by the BELLE Collaboration through the process $e^+e^- \rightarrow \Upsilon(5S) \rightarrow h_b(nP) + \pi^+\pi^-$ [3].

The quite accurate measurements of the mass of the h_c (also $h_b(1P, 2P)$) implies a rather small P -wave hyperfine mass splitting. This is theoretically intriguing since it might be able to impose some severe constraint on the quark spin-spin interaction as well as possible charm meson loop effect.

Aside from its mass [4, 5], our knowledge about the h_c state is still quite limited. The h_c appears to be a narrow resonance with the total width of $0.73 \pm 0.45 \pm 0.28$ MeV [5]. By far two decay channels of the h_c have been seen, one is the hadronic decay $h_c \rightarrow 2(\pi^+\pi^-)\pi^0$ [6], and the other is the $E1$ transition $h_c \rightarrow \eta_c\gamma$, both of which have comparable partial widths. Recently BES III experiment has measured the absolute branching fraction of the latter process and gives $\mathcal{B}(h_c \rightarrow \gamma\eta_c) = (54.3 \pm 6.7 \pm 5.2)\%$. It seems that these two decay channels have already constituted the bulk of the full width of the h_c .

In contrast to the decay, our understanding of the h_c production is even poorer. The only measurement of the h_c production is from a recent CLEO experiment, by observing the process $e^+e^- \rightarrow h_c\pi^+\pi^-$ at $\sqrt{s} = 4.170$ GeV [7]. On the theoretical side, rather few work on h_c production are scattered in literature. Among these studies, are h_c production in B meson inclusive decay [8, 9], h_c photoproduction [10], h_c hadroproduction [11, 12]. It is interesting to compare this situation with highly intensive studies on J/ψ production in various collision experiments [13].

Our goal in this work is to carry out a detailed study on inclusive h_c production in e^+e^- annihilation, which is specifically relevant to the B factories experiments. Specifically, we investigate the inclusive production of the h_c meson associated both with light hadrons and with charmed hadrons. There are both theoretical and experimental merits to study these processes. On the theoretical side, since these processes are much simpler than the h_c production in hadronic collision, one expects to obtain more precise prediction with less contamination from the nonperturbative side of QCD. On the experimental side, since e^+e^- collision experiment possesses much clean background than the hadronic collider, and B factories have already accumulated a quite large data sample near the $\Upsilon(4S)$ resonance, it could well be the most likely place to unambiguously observe the elusive h_c signal.

Our study is based on the nonrelativistic QCD (NRQCD) factorization, a widely-accepted framework to deal with inclusive quarkonium production [14]. Nowadays NRQCD factorization has superseded the obsolete color-singlet model and color evaporation model as a modern and model-independent approach. A highlight of this approach is the color-octet mechanism, which is an indispensable ingredient in order to give a meaningful prediction for the P wave quarkonium production [9].

As we will see, for the process $e^+e^- \rightarrow h_c + \text{light hadrons}$, the color-octet mechanism indeed plays a pivotal role in rendering infrared-finite prediction for the inclusive h_c production rate. Furthermore, this process is found to be dominated by the color-octet channel. Our study reveals that this process may have a sizable total cross section that is comparable

in magnitude with that of $e^+e^- \rightarrow J/\psi + \text{light hadrons}$, which has been measured some time ago by B factory experiments [15]. Future measurement of this process at B factories may provide an explicit test on the color-octet mechanism, as well as put useful constraint on the value of the color-octet matrix element for h_c ¹.

The rest of the paper is organized as follows. In Sec. II, we present the NRQCD factorization formulas for h_c inclusive production in e^+e^- annihilation, accurate at lowest order in v . In Sec. III, by employing the perturbative matching ansatz, we determine the infrared-finite color-singlet and color-octet short-distance coefficients associated with the process $e^+e^- \rightarrow h_c + \text{light hadrons}$. In Sec. IV, we determine the color-singlet and color-octet short-distance coefficient associated with the process $e^+e^- \rightarrow h_c + \text{charmed hadrons}$. Based on our calculation in previous sections, we devote Sec. V to exploring the observation prospects of h_c production at B factories. Finally we summarize in Sec. VI. In Appendix A, we explain some technical details in isolating the infrared divergence for $e^+e^- \rightarrow h_c + gg$ in dimensional regularization. In Appendix B, we present the color-singlet short-distance coefficient for the process $e^+e^- \rightarrow \eta_c + c\bar{c}$.

II. NRQCD FACTORIZATION FORMULA FOR h_c PRODUCTION

NRQCD factorization formalism is a systematic tool for analyzing the inclusive production of heavy quarkonium [14]. The production rate can be expressed as a sum of products of short-distance coefficients and nonperturbative, albeit universal vacuum NRQCD matrix elements, whose importance is organized by the typical quark velocity, v . In this work, we will consider $e^+e^- \rightarrow h_c + X$ in this factorization framework. At the lowest order in v , the velocity counting rule implies that the cross section of h_c has the following form:

$$d\sigma[e^+e^- \rightarrow h_c + X] = \frac{dF_1}{m_c^4} \langle \mathcal{O}_1^{h_c}(^1P_1) \rangle + \frac{dF_8}{m_c^2} \langle \mathcal{O}_8^{h_c}(^1S_0) \rangle, \quad (1)$$

where the color-singlet operator $\mathcal{O}_1^{h_c}(^1P_1)$ and the color-octet operator $\mathcal{O}_8^{h_c}(^1S_0)$ have been introduced in [14]. It is interesting to contrast this P -wave quarkonium production process with the S -wave onium production, where the color-octet operator matrix element first comes into play only at relative $O(v^4)$.

dF_1, dF_8 are infrared-finite short-distance coefficients associated with the vacuum matrix elements of color-singlet and octet NRQCD production operators. Since they are insensitive to the long-distance strong interaction dynamics, a standard way of determining them is through the perturbative matching procedure: replacing the h_c state appearing in (1) with the free on-shell $c\bar{c}(n)$ states ($n = ^1S_0^{(8)}$ or $^1P_1^{(1)}$), and computing both sides of (1) using perturbative QCD and perturbative NRQCD, respectively, then enforcing that they generate identical results. Finally, one then solves two linear equations to identify two unknown coefficients, order by order in α_s ².

¹ The majority of the results in this paper has already been presented in Ref. [16].

² In this work, we are only looking for the h_c energy distribution and total cross section, rather than its angular distribution. To this purpose, we may adopt a standard shortcut to simplify the intermediate calculations [17]. First compute the virtual photon decay into h_c , then use the following formula to convert the decay rate into h_c cross section: $d\sigma[e^+e^- \rightarrow h_c(P) + X]/dP^0 = \frac{4\pi\alpha}{s^{3/2}} d\Gamma[\gamma^* \rightarrow h_c(P) + X]/dP^0$, where P^μ represents the 4-momentum of the h_c in the e^+e^- center-of-mass frame.

The perturbative matching for $e^+e^- \rightarrow h_c +$ charmed hadrons are straightforward. In contrast, the matching procedure for $e^+e^- \rightarrow h_c +$ light hadrons is more subtle and involved, since the QCD side calculation for the color-singlet channel $d\sigma[e^+e^- \rightarrow c\bar{c}(^1P_1^{(1)}) + gg]$ contains infrared divergence, which must be absorbed into the color-octet matrix element to render an infrared finite color-singlet short-distance coefficient.

III. h_c PRODUCTION ASSOCIATED WITH LIGHT HADRONS

In this section, we will apply the perturbative matching procedure to deduce the short-distance coefficients for inclusive h_c production associated with light hadrons at B factories, i.e., $e^+e^- \rightarrow h_c +$ light hadrons. For clarity, we will always attach a superscript ‘‘LH’’ to both F_1 and F_8 in this section, to differentiate them from the analogous coefficients for the h_c production associated with charmed hadrons, which will be reported in the next section.

A. Determining dF_8^{LH}

We begin with calculating the differential short-distance coefficient dF_8^{LH} affiliated with the color-octet operator. At the lowest order in α_s , only two Feynman diagrams need to be considered for the process $e^+e^- \rightarrow c\bar{c}(^1S_0^{(8)}) + g$.

As mentioned before, the differential cross section $d\sigma[e^+e^- \rightarrow c\bar{c}(^1P_1) + gg]/dz$ would develop an IR divergence as one of the gluons gets soft. In order to deduce the IR finite color-singlet coefficient dF_1^{LH} , the perturbative factorization formula (1) implies that we should also consider the color-octet coefficient dF_8 multiplied by the renormalized $O(\alpha_s)$ color-octet matrix element, which is generally IR divergent. Throughout this work we find it most convenient to employ the dimensional regularization (DR) to regularize both UV and IR divergences. Therefore, it is necessary to compute $e^+e^- \rightarrow c\bar{c}(^1S_0^{(8)}) + g$ in $D = 4 - 2\epsilon$ spacetime dimensions.

It is convenient to use the covariant spin projection method [18] to compute the amplitude of $\gamma^* \rightarrow c\bar{c}(^1S_0^{(8)}) + g$ in D dimensions. A subtlety is that the appearance of γ_5 from the spin-singlet projector, which requires some care to handle it in $D = 4 - 2\epsilon$ dimension. For consistency, we adopt the ’t Hooft-Veltman (HV) prescription [19], and utilize West’s formula to calculate the trace of one γ_5 and a string of Dirac matrices [20]. The Levi-Civita tensor is assumed as a 4-dimensional object ³.

We will always work in the e^+e^- center-of-mass frame throughout this paper, where \sqrt{s} denotes the e^+e^- center-of-mass energy. For notational simplicity, we define the energy fraction of h_c , $z \equiv 2P^0/\sqrt{s}$, as well as the ratio of charm quark mass over center-of-mass energy, $r \equiv 4m_c^2/s$. The differential two-body phase space in $D = 4 - 2\epsilon$ dimensions can be expressed as

$$d\Phi_2 = \frac{C_\epsilon}{8\pi} s^{-\epsilon} (1-r)^{1-2\epsilon} \delta(1+r-z) dz, \quad (2)$$

³ As a crosscheck, we have also tried to treat the Levi-Civita tensor as a D -dimensional object when computing the squared amplitude. After matching is done, one is justified to return to 4 dimensions. It turns out that this alternative prescription leads to the identical short-distance coefficients dF_8 and dF_1 , as given in (4) and (17) in the text.

where $c_\epsilon = (4\pi)^\epsilon \frac{\Gamma(1-\epsilon)}{\Gamma(2-2\epsilon)}$.

Comparing both sides of (1) at $O(\alpha_s)$, it is easy to find the differential coefficient dF_8^{LH} in $4 - 2\epsilon$ dimensions:

$$\frac{dF_8^{\text{LH}}}{dz} = c_\epsilon \left(\frac{\mu^2}{s} \right)^\epsilon \frac{32\pi^2 e_c^2 \alpha^2 \alpha_s m_c}{3s^2} (1-r)^{1-2\epsilon} \delta(1+r-z), \quad (3)$$

where μ is the compensating mass scale in DR, $e_c = \frac{2}{3}$ is the electric charge of charm quark.

If taking $\epsilon \rightarrow 0$, the differential color-octet coefficient reduces to

$$\frac{dF_8^{\text{LH}}}{dz} = \frac{32\pi^2 e_c^2 \alpha^2 \alpha_s m_c}{3s^2} (1-r) \delta(1+r-z). \quad (4)$$

B. Determining dF_1^{LH}

We proceed to determine the color-singlet coefficient for h_c production associated with light hadrons in e^+e^- annihilation, dF_1^{LH} . This can be expedited by replacing the h_c state with a free $c\bar{c}(^1P_1^{(1)})$ pair, and matching both sides of (1) that are computed in perturbative QCD and perturbative NRQCD, respectively.

At the lowest order in α_s , the color-singlet h_c production associated with light hadrons can proceed through the parton-level process $e^+e^- \rightarrow c\bar{c}(^1P_1^{(1)})gg$, which can be picturized by six Feynman diagrams. Let P, k_1, k_2 signify the momenta of the $c\bar{c}(^1P_1^{(1)})$ pair, gluon 1, and gluon 2, respectively. We will always assume $P^2 \approx 4m_c^2$. It is convenient to introduce three fractional energy variables z, x_1 and x_2 :

$$z = \frac{2P^0}{\sqrt{s}}, \quad x_1 = \frac{2k_1^0}{\sqrt{s}}, \quad x_2 = \frac{2k_2^0}{\sqrt{s}}, \quad (5)$$

which are subject to the constraint $x_1 + x_2 + z = 2$, as required by the energy conservation.

Since we employ the DR to regularize the potential IR divergences, it is useful to write down the 3-body phase space integral in $4 - 2\epsilon$ spacetime dimensions:

$$\int d\Phi_3 = \frac{c_\epsilon (4\pi)^\epsilon}{\Gamma(1-\epsilon)} \left(\frac{s}{2} \right)^{1-2\epsilon} \frac{1}{(4\pi)^3} \int_{2\sqrt{r}}^{1+r} dz \int_{x_1^-}^{x_1^+} dx_1 x_1^{-2\epsilon} (z^2 - 4r)^{-\epsilon} (1 - \cos^2\theta)^{-\epsilon}, \quad (6)$$

where θ signifies the angle between \mathbf{P} and \mathbf{k}_1 in the γ^* rest frame. For given z and x_1 , it can be uniquely determined:

$$\cos\theta = \frac{2(1+r-z) - x_1(2-z)}{x_1\sqrt{z^2 - 4r}}. \quad (7)$$

Since we have taken the shortcut by first calculating the virtual photon decay into 3-body final states, only two independent energy fraction variables need be retained in the integration measure in (6). The integration limits of z have been explicitly labeled in (6), while the integration boundaries of x_1, x_1^\pm , are parameterized as $a(z) \pm b(z)$, where

$$a(z) = \frac{1}{2}(2-z), \quad (8a)$$

$$b(z) = \frac{1}{2}\sqrt{z^2 - 4r}. \quad (8b)$$

We again use the spin projection technique [18] to compute the amplitude of $\gamma^* \rightarrow c\bar{c}(^1P_1^{(1)}) + gg$ in D dimension and use the HV prescription to handle the trace involving γ_5 . After squaring the amplitude and summing over polarizations and colors, we separate the squared amplitudes into two pieces:

$$\sum_{\text{Pol, Col}} \left| \mathcal{A}[\gamma^* \rightarrow c\bar{c}(^1P_1^{(1)}) + gg] \right|^2 = I_{\text{div}}(x_1, z) + I_{\text{fin}}(x_1, z), \quad (9)$$

where

$$I_{\text{div}}(x_1, z) = \frac{2^{16}\pi^3 e_c^2 \alpha C_F \alpha_s^2 \mu^{4\epsilon}}{s^2} (1 - \epsilon) \left[\frac{1}{(1+r-z-x_1)^2} + \frac{1}{(1+r-z-x_2)^2} \right] \quad (10)$$

represents the term that would bring forth an IR singularity when integrating over two distinct phase space corners: $z \rightarrow 1+r, x_1 \rightarrow 0$ and $z \rightarrow 1+r, x_2 \rightarrow 0$, where one of the gluons become soft. The symbol I_{fin} denotes the remainder of the squared amplitude which contains no terms as dangerous as those in (10), therefore renders a finite result upon integrating over the entire 3-body phase space. Bose symmetry guarantees that I_{fin} is manifestly symmetric under interchange between x_1 and $x_2 = 2 - z - x_1$. Since its explicit expression is somewhat lengthy, so will not be reproduced here.

Accordingly, the energy distribution of the parton cross section can also be decomposed into two parts:

$$\frac{d\sigma[e^+e^- \rightarrow c\bar{c}(^1P_1^{(1)}), P) + gg]}{dz} = \frac{d\hat{\sigma}_{\text{div}}}{dz} + \frac{d\hat{\sigma}_{\text{fin}}}{dz}, \quad (11)$$

which are obtained by integrating (9) over the entire momentum range of gluon 1:

$$\int_{2\sqrt{r}}^{1+r} dz \frac{d\hat{\sigma}_{\text{div}}}{dz} = \frac{\pi\alpha}{3s^2} \int d\Phi_3 I_{\text{div}}(x_1, z), \quad (12a)$$

$$\int_{2\sqrt{r}}^{1+r} dz \frac{d\hat{\sigma}_{\text{fin}}}{dz} = \frac{\pi\alpha}{3s^2} \int d\Phi_3 I_{\text{fin}}(x_1, z). \quad (12b)$$

In deriving these, we have used the conversion formula explained in footnote 2, as well as included a $\frac{1}{2!}$ factor to account for the indistinguishability of two gluons in the final state.

It is straightforward to complete the integration over x_1 in the right side of (12b). Since everything is finite, this integral can be directly calculated in 4 dimensions. In contrast, integrating I_{div} over x_1 in DR requires some special care due to emergence of the IR divergence that occurs at $z = 1+r$. We devote Appendix A to expounding the intermediate

technical steps, and here just simply jump to the desired results:

$$\begin{aligned} \frac{d\hat{\sigma}_{\text{div}}}{dz} = & \frac{128\pi e_c^2 \alpha^2 C_F \alpha_s^2}{3m_c^2 s^2} \frac{c_\epsilon (4\pi)^\epsilon}{\Gamma(1-\epsilon)} \left\{ (1-r)\delta(1+r-z) \times \right. \\ & \left(-\frac{1}{\epsilon_{\text{IR}}} - 2 \ln \frac{\mu^2}{4m_c^2} + 2 \ln \frac{(1-\sqrt{r})^2}{\sqrt{r}} + 1 \right) + \left[\frac{1}{1+r-z} \right]_+ \left(\frac{z^2-4r}{z-2r} + \sqrt{z^2-4r} \right) \\ & \left. + \frac{2z}{z-2r} - \frac{2-z-\sqrt{z^2-4r}}{1+r-z} \right\}, \end{aligned} \quad (13a)$$

$$\begin{aligned} \frac{d\hat{\sigma}_{\text{fin}}}{dz} = & \frac{256\pi e_c^2 \alpha^2 C_F \alpha_s^2}{3m_c^2 s^2} \frac{1}{(2-z)^4 (z-2r)^5} \left\{ (z-2r)\sqrt{z^2-4r} \times \right. \\ & \left[16r(-3+2r-6r^2-6r^3+3r^4+6r^5) + 16r(7+2r+24r^2+r^3-20r^4-2r^5)z \right. \\ & + 4(2-35r-72r^2-74r^3+94r^4+25r^5)z^2 - 8(2-21r-34r^2+18r^3+15r^4)z^3 \\ & \left. + 2(3-59r-6r^2+32r^3)z^4 + (3+23r-14r^2)z^5 - z^6 \right] \\ & + \ln \frac{z-2r+\sqrt{z^2-4r}}{z-2r-\sqrt{z^2-4r}} \left[-32r^2(3-r+4r^2+3r^3+2r^5+5r^6) \right. \\ & + 32r^2(8+r+14r^2+4r^3+6r^4+21r^5+2r^6)z \\ & + 8r(4-37r-31r^2-54r^3-38r^4-149r^5-31r^6)z^2 \\ & - 8r(12-25r-26r^2-42r^3-148r^4-51r^5)z^3 \\ & + 2r(61-17r-55r^2-363r^3-186r^4)z^4 - 12r(8+2r-21r^2-17r^3)z^5 \\ & \left. \left. + (1+45r-37r^2-65r^3)z^6 - (1+5r-10r^2)z^7 \right] \right\}. \end{aligned} \quad (13b)$$

The appearance of the δ -function and “+”-function exhibits some peculiarity of the energy distribution $d\hat{\sigma}_{\text{div}}/dz$ near the maximal h_c energy. As usual, these functions should be interpreted as the distributions in the mathematical sense. The $[f(z)]_+$ function in (13a) is defined such that when convoluting it with an arbitrary function $g(z)$ that is regular at $z = 1+r$, one gets

$$\int_{2\sqrt{r}}^{1+r} dz [f(z)]_+ g(z) = \int_{2\sqrt{r}}^{1+r} dz f(z) (g(z) - g(1+r)). \quad (14)$$

From (13a), we find that the IR singularity is exactly located at the maximal value of z . One certainly expects that this IR singularity will be swept out once including the color-octet contribution. Encouragingly, equation (3) implies that the differential color-octet coefficient dF_8^{LH} is also proportional to a peaked distribution $\delta(1+r-z)$.

Since dF_8^{LH}/dz is of order α_s only, in order to match the $O(\alpha_s^2)$ accuracy of the color-singlet parton cross section, we need incorporate the $O(\alpha_s)$ correction to the perturbative color-octet NRQCD matrix element. This correction has already been inferred previously

in the related work on quarkonium production, so we just present the result ⁴:

$$\langle \mathcal{O}_8^{c\bar{c}}(^1S_0) \rangle_{\overline{\text{MS}}} = \langle \mathcal{O}_8^{c\bar{c}}(^1S_0) \rangle^{(0)} - \frac{2C_F\alpha_s}{3N_c\pi m_c^2} \left(\frac{1}{\epsilon_{\text{IR}}} + \ln 4\pi - \gamma_E \right) \langle \mathcal{O}_1^{c\bar{c}}(^1P_1) \rangle^{(0)} + \dots, \quad (15)$$

where $C_F = \frac{N_c^2-1}{2N_c}$, and $N_c = 3$ is the number of the colors in QCD. Under renormalization, the color-octet operator $\mathcal{O}_8^{c\bar{c}}(^1S_0)$ mixes with the color-singlet operator $\mathcal{O}_1^{c\bar{c}}(^1P_1)$ (it also mixes with the color-octet operator $\mathcal{O}_8^{c\bar{c}}(^1P_1)$, but whose effect would arise at higher order in v). It is important to note that, the $\overline{\text{MS}}$ -renormalized perturbative matrix element $\langle \mathcal{O}_8^{c\bar{c}}(^1S_0) \rangle$ develops a logarithmic IR divergence.

In passing, it may be worth stressing that, unlike the NRQCD decay operators, the analogous production operators are no longer the local 4-fermion operators. In fact, in a series of work [21–23], Nayak, Qiu and Sterman have recently advocated that one must insert the proper gauge links to the original definitions of the color-octet production operators [14] to warrant the gauge invariance, and the nontrivial effect due to this gauge completion first shows up at next-to-next-to-leading in α_s (it has also been explicitly examined that, at the NLO in α_s , forgoing the gauge completion for the color-octet operators does not bring in any inconsistency [24]). Thus to our purpose, we are content with staying with the original definition given in [14]. In this respect, equation (15) looks very similar to the analogous formula for the renormalized color-octet decay operator in NRQCD [18, 25].

In light of the matching condition in (1) for the $c\bar{c}(^1P_1^{(1)})$ channel, one can write down the following equation for dF_1^{LH} to the order α_s^2 :

$$\begin{aligned} \frac{d\sigma[e^+e^- \rightarrow c\bar{c}(^1P_1^{(1)}) + gg]}{dz} &= \frac{6N_c}{m_c^3} \frac{dF_1^{\text{LH}}(\mu)}{dz} - \frac{128\pi e_c^2 \alpha^2 C_F \alpha_s^2 (1-r)}{3m_c^2 s^2} \times \\ c_\epsilon \left[\frac{1}{\epsilon_{\text{IR}}} + \ln \frac{\pi\mu^2}{m_c^2} - \gamma_E + \ln r - 2\ln(1-r) - \frac{2}{3} \right] &\delta(1+r-z), \end{aligned} \quad (16)$$

where we have explicitly substituted the LO color-octet coefficient in (3) and the NLO correction to the color-octet matrix element (15).

Substituting the analytic expressions for the differential $c\bar{c}(^1P_1^{(1)})$ production cross section, as assembled in (13), into (16), one can readily solve the desired differential color-singlet coefficient:

$$\begin{aligned} \frac{dF_1^{\text{LH}}(\mu)}{dz} &= \frac{64\pi e_c^2 \alpha^2 C_F \alpha_s^2 m_c}{9N_c s^2} \left\{ \left(-\ln \frac{\mu^2}{4m_c^2} + 2\ln \frac{1-\sqrt{r}}{1+\sqrt{r}} + \frac{1}{3} \right) \times \right. \\ (1-r)\delta(1+r-z) &+ \left[\frac{1}{1+r-z} \right]_+ \left(\frac{z^2-4r}{z-2r} + \sqrt{z^2-4r} \right) \\ &\left. + \frac{2z}{z-2r} - \frac{2-z-\sqrt{z^2-4r}}{1+r-z} \right\} + \frac{m_c^3}{6N_c} \frac{d\hat{\sigma}_{\text{fin}}}{dz}, \end{aligned} \quad (17)$$

⁴ Note the authors of Ref. [8] used DR to regularize the UV divergence but a gluon mass to regulate the IR divergence for the perturbative color-octet NRQCD matrix element. Here we use DR to regulate both UV and IR divergences.

where $d\hat{\sigma}_{\text{fin}}/dz$ has been given in (13b). Although this short-distance coefficient is now free of IR singularity, as it should, it now depends logarithmically on the NRQCD factorization scale μ . However, when taking into account the μ -dependence of the color-octet matrix element $\langle \mathcal{O}_8^{h_c}(^1S_0) \rangle$, the physical h_c production rate in (1) in principle does not depend on this artificial scale.

C. The integrated short-distance coefficients F_1^{LH} and F_8^{LH}

Inspecting the differential coefficients in (4) and (17), one finds that the distribution of h_c becomes singular near its maximum energy. However, it was noticed long ago that NRQCD expansion breaks down near the kinematic boundary of quarkonium momentum distribution [26], thus the NRQCD prediction at fixed order is no longer trustworthy. In order to reliably describe the energy distribution near the kinematic end point, one should incorporate the effect of nonperturbative shape function [27], as well as resum large Sudakov logarithm [28], consequently the quarkonium spectrum near the endpoint will turn over and get smeared. However, including such refinement is beyond the scope of this work, which well deserves a dedicated study.

On the other hand, the integrated h_c production rate is much less sensitive to the above-mentioned effects, and NRQCD velocity expansion is believed to work well for this quantity. Moreover, the total production rate of the h_c is also experimentally accessible. Therefore, it is of phenomenological incentive to find the integrated short-distance coefficients F_1^{LH} and F_8^{LH} .

Integrating (17) over z may seem straightforward, but it turns out to be difficult to obtain the analytic expression for the part involving $d\hat{\sigma}_{\text{fin}}/dz$. We utilize a simple trick [29], i.e., restarting from (12b), but this time integrating over z first, then followed by integrating over x_1 . After some algebra, we end up with the following integrated short-distance coefficients:

$$F_1^{\text{LH}}(\mu) = \frac{64\pi e_c^2 \alpha^2 C_F \alpha_s^2 m_c}{9N_c s^2} (1-r) \left[-\ln \frac{\mu^2}{4m_c^2} + 2\ln(1-r) - \frac{65-84r}{12(1-r)} \right. \\ \left. + \frac{7+7r-9r^2}{6(1-r)^2} \ln r + \frac{r(5-7r) \ln^2 \frac{1+\sqrt{1-r}}{1-\sqrt{1-r}}}{16(1-r)^2} + \frac{(14-15r) \ln \frac{1+\sqrt{1-r}}{1-\sqrt{1-r}}}{8(1-r)^{3/2}} \right], \quad (18a)$$

$$F_8^{\text{LH}} = \frac{32\pi^2 e_c^2 \alpha^2 \alpha_s m_c}{3s^2} (1-r). \quad (18b)$$

The color-octet coefficient F_8^{LH} can be trivially deduced by integrating (4) over z .

It is natural to take the factorization scale μ around m_c . We then find that $F_1^{\text{LH}}(\mu)$ becomes negative in most of the allowed range of r (including $r \approx 0.08$ of phenomenological interest), except in a narrow window where r is very small. This has an immediate consequence, that the color-octet channel becomes indispensable if one wishes to predict a *positive* total production rate for $e^+e^- \rightarrow h_c + \text{light hadrons}$.

It is enlightening to examine the asymptotic behaviors of (18) in the limit $\sqrt{s} \gg m$:

$$F_1^{\text{LH}}(\mu) \Big|_{\text{asym}} = \frac{64\pi e_c^2 \alpha^2 C_F \alpha_s^2 m_c}{9N_c s^2} \left[-\frac{7}{12} \ln r - \ln \frac{\mu^2}{4m_c^2} - \frac{65}{12} + \frac{7}{2} \ln 2 \right], \quad (19a)$$

$$F_8^{\text{LH}} \Big|_{\text{asym}} = \frac{32\pi^2 e_c^2 \alpha^2 \alpha_s m_c}{3s^2}. \quad (19b)$$

The total production rate for $e^+e^- \rightarrow h_c + \text{light hadrons}$ scales with the center-of-mass energy as $1/s^2$, which is the same as that for $e^+e^- \rightarrow J/\psi + \text{light hadrons}$ [29]. Nevertheless, it is interesting to note that the leading scaling violation in (19a) is represented by a single-logarithmic term ($\propto \ln r$), while that in the $e^+e^- \rightarrow J/\psi + gg$ process is by a double-logarithmic term ($\propto \ln^2 r$) [29]. Since the newly developed perturbative QCD factorization formalism for quarkonium production [30] is based on m_c^2/s expansion, it is natural to envisage that refactorizing the higher-twist two-parton fragmentation function in [30] may provide a natural framework to identify these logarithms at $O(\alpha_s^2)$ and resum them to all orders in α_s .

IV. h_c PRODUCTION ASSOCIATED WITH CHARMED HADRONS

In this section, we investigate inclusive h_c production associated with charmed hadrons at B factories, i.e., $e^+e^- \rightarrow h_c + X_{c\bar{c}}$. Our central task is again to infer two short-distance coefficients appearing in the NRQCD factorization formula (1). To avoid confusion, we will always associate a superscript ‘‘Charm’’ to F_1 and F_8 in this section, to distinguish from the analogous coefficients associated with the process $e^+e^- \rightarrow h_c + \text{light hadrons}$ in Sec. III.

Both color-singlet and octet channels first occur at $O(\alpha_s^2)$, characterized with the parton processes $e^+e^- \rightarrow c\bar{c}(^1P_1^{(1)}, ^1S_0^{(8)}) + c\bar{c}$. Since both channels share the common parton kinematics, we list some useful 3-body phase-space formulas here.

We denote the momenta of the $c\bar{c}$ pair, c , and \bar{c} by P , k_1 , k_2 , respectively, with $P^2 \approx 4m_c^2$, $k_1^2 = k_2^2 = m_c^2$. Analogous to (5), we also introduce three fractional energy variables z , x_1 and x_2 , which are subject to the constraint $x_1 + x_2 + z = 2$.

Since no massless particles are involved in the final state, the parton cross sections in both channels do not exhibit any IR singularity. Unlike in Sec. III, we thus can perform the calculation directly in 4 spacetime dimensions. Consequently, suffice it to give the 4-dimensional 3-body phase space measure for the process $\gamma^* \rightarrow c\bar{c}(P) + c(k_1) + \bar{c}(k_2)$:

$$\int d\Phi_3 = \frac{s}{128\pi^3} \int_{2\sqrt{r}}^1 dz \int_{x_1^-}^{x_1^+} dx_1. \quad (20)$$

The integration limits of z have been explicitly specified, while those for the fractional energy of c , x_1^\pm , read

$$x_1^\pm = \frac{2-z}{2} \pm \frac{1}{2} \sqrt{\frac{(1-z)(z^2-4r)}{1+r-z}}. \quad (21)$$

A. Deducing dF_1^{Charm}

We start with calculating the differential color-singlet coefficient dF_1^{Charm} . At the lowest order in α_s , only four Feynman diagrams need to be considered for the process $\gamma^* \rightarrow c\bar{c}(^1P_1^{(1)}) + c\bar{c}$. This calculation is quite similar to the analogous one for $e^+e^- \rightarrow J/\psi + c\bar{c}$ [31] and $e^+e^- \rightarrow \chi_{cJ}(\eta_c) + c\bar{c}$ ($J = 0, 1, 2$) [32]. The perturbative matching calculation for this

coefficient is rather straightforward, so we directly present the result:

$$\begin{aligned}
\frac{dF_1^{\text{Charm}}}{dz} = & \frac{64\pi e_c^2 \alpha^2 \alpha_s^2}{243m_{cs}(2-z)^4 z^4} \left\{ \frac{\sqrt{(1+r-z)(1-z)(z^2-4r)}}{(2-z)^4} \left[768r^4 - 384r^3(8+5r)z \right. \right. \\
& -64r(8-16r-128r^2-35r^3)z^2 + 32r(56-64r-310r^2-43r^3)z^3 \\
& +16(8-140r+136r^2+438r^3+25r^4)z^4 - 8(48-80r+136r^2+336r^3-15r^4)z^5 \\
& +4(152+164r-112r^2+132r^3-7r^4)z^6 - (672+560r-400r^2+84r^3-6r^4)z^7 \\
& \left. +2(300+182r-60r^2-r^3)z^8 - 8(49+14r-2r^2)z^9 + (130+17r)z^{10} - 18z^{11} \right] \\
& - \frac{r}{2z} \ln \frac{z\sqrt{1+r-z} + \sqrt{(1-z)(z^2-4r)}}{z\sqrt{1+r-z} - \sqrt{(1-z)(z^2-4r)}} \times \\
& \left[-192r^4 + 96r^3(8+3r)z + 32r(4-8r-39r^2-6r^3)z^2 - 32r(10-4r-26r^2-r^3)z^3 \right. \\
& -4(8-132r-44r^2+48r^3+5r^4)z^4 + 2(48-192r-64r^2+48r^3+3r^4)z^5 \\
& \left. -2(72+36r+82r^2+11r^3)z^6 + 4(38+61r+13r^2)z^7 - (90+59r)z^8 + 16z^9 \right] \left. \right\}. \quad (22)
\end{aligned}$$

B. Deducing dF_8^{Charm}

Next we proceed to calculate the differential color-octet coefficient dF_8^{Charm} . At the order α_s^2 , we need consider six Feynman diagrams for the parton process $\gamma^* \rightarrow c\bar{c}(^1S_0^{(8)}) + c\bar{c}$. The perturbative matching for this coefficient is analogous to that in Sec. III A, which is also quite straightforward. Here we just give the result:

$$\begin{aligned}
\frac{dF_8^{\text{Charm}}}{dz} = & \frac{\pi e_c^2 \alpha^2 \alpha_s^2}{27m_{cs}} \frac{1}{(1+r-z)(2-z)^2 z^3} \left\{ \frac{2z\sqrt{(1-z)(z^2-4r)}}{3(2-z)^4(1+r-z)^{3/2}} \times \right. \\
& \left[96r^3(1+r)^3 - 96r^2(1+r)^2(4+8r+r^2)z \right. \\
& +16(6+59r+186r^2+328r^3+284r^4+51r^5-2r^6)z^2 \\
& -8(48+374r+770r^2+965r^3+551r^4+41r^5-r^6)z^3 \\
& +(592+3392r+5556r^2+5806r^3+2234r^4+90r^5-6r^6)z^4 \\
& -2(232+704r+1162r^2+1131r^3+244r^4-5r^5)z^5 \\
& +(262-207r+217r^2+293r^3+11r^4)z^6 - (184-397r-186r^2-15r^3)z^7 \\
& \left. + (116-139r-40r^2)z^8 - (40-13r)z^9 + 6z^{10} \right] + r \ln \frac{z\sqrt{1+r-z} + \sqrt{(1-z)(z^2-4r)}}{z\sqrt{1+r-z} - \sqrt{(1-z)(z^2-4r)}} \times \\
& \left[8r^3(1+r) - 8r^2(4+5r)z - 2(4-2r-22r^2-r^3-r^4)z^2 \right. \\
& \left. + (8+8r+40r^2-6r^3)z^3 - (14+33r-5r^2)z^4 + (2-19r)z^5 + 12z^6 \right] \left. \right\}. \quad (23)
\end{aligned}$$

C. Fragmentation function for $c \rightarrow h_c$ and integrated cross section

At first sight, the differential coefficients in (22) and (23) may look too disordered to extract anything useful. However, this is just a disguise, since we are certain that in the asymptotic limit $\sqrt{s} \gg m_c$, the differential h_c production rate associated with $c\bar{c}$ must be dominated by the fragmentation mechanism:

$$\frac{d\sigma[e^+e^- \rightarrow h_c(P) + X_{c\bar{c}}]}{dz} = 2\check{\sigma}D_{c \rightarrow h_c}(z), \quad (24)$$

where $\check{\sigma} = N_c \frac{4\pi e_c^2 \alpha^2}{3s}$ is the cross section for the process $e^+e^- \rightarrow c\bar{c}$, and $D_{c \rightarrow h_c}(z)$ stands for the fragmentation probability for c into the h_c carrying the energy fraction z . The factor 2 arises because both c and \bar{c} can fragment into h_c with equal probability.

According to the NRQCD factorization, the fragmentation function of c into h_c can be refactorized as

$$D_{c \rightarrow h_c}(z) = d_1^{h_c}(z) \frac{\langle \mathcal{O}_1^{h_c}(^1P_1) \rangle}{m_c^5} + d_8^{h_c}(z) \frac{\langle \mathcal{O}_8^{h_c}(^1S_0) \rangle}{m_c^3}, \quad (25)$$

where $d_1^{h_c}(z)$ and $d_8^{h_c}(z)$ are the corresponding short-distance coefficient (jet) functions.

Comparing (24) with (1), one can immediately realize that, these short-distance functions can be obtained by taking the asymptotic ($r \rightarrow 0$) limit of dF_n^{Charm}/dz ($n = 1, 8$):

$$\begin{aligned} d_1^{h_c}(z) &= \left. \frac{m_c}{2\check{\sigma}} \frac{dF_1^{\text{Charm}}}{dz} \right|_{\text{asym}} \\ &= \frac{16\alpha_s^2 z(1-z)^2 (64 - 128z + 176z^2 - 160z^3 + 140z^4 - 56z^5 + 9z^6)}{243(2-z)^8}, \end{aligned} \quad (26a)$$

$$d_8^{h_c}(z) = \left. \frac{m_c}{2\check{\sigma}} \frac{dF_8^{\text{Charm}}}{dz} \right|_{\text{asym}} = \frac{\alpha_s^2 z(1-z)^2 (48 + 8z^2 - 8z^3 + 3z^4)}{162(2-z)^6}. \quad (26b)$$

Both the expressions for $d_1^{h_c}(z)$ and $d_8^{h_c}(z)$ in (26) fully agree with Ref. [33].

Honestly speaking, the B factory energy is far from being asymptotically large. Therefore for this phenomenologically relevant case, the fragmentation function calculated in (26) can hardly faithfully reproduce the energy distribution of the h_c depicted in (22) and (23).

Like what has been done in Sec. III C, it is also of both theoretical and phenomenological interest in knowing the integrated production rate for $e^+e^- \rightarrow h_c +$ charmed hadrons. Conceivably, it seems extremely challenging, if not impossible, to complete the integration of (22) and (23) over z in closed form. Nevertheless, it is quite easy to infer the asymptotic behavior of the total cross section with the help of the fragmentation function:

$$\begin{aligned} \sigma[e^+e^- \rightarrow h_c + X_{c\bar{c}}] \Big|_{\text{asym}} &= 2\check{\sigma} \int_0^1 dz D_{c \rightarrow h_c}(z) \\ &= 16\alpha_s^2 \check{\sigma} \left[\frac{18107 - 26110 \ln 2}{8505} \frac{\langle \mathcal{O}_1^{h_c}(^1P_1) \rangle}{m_c^5} + \frac{773 - 1110 \ln 2}{12960} \frac{\langle \mathcal{O}_8^{h_c}(^1S_0) \rangle}{m_c^3} \right]. \end{aligned} \quad (27)$$

In contrast to (19), the production rate for $h_c +$ charmed hadron exhibits much slower asymptotic decrease ($\propto 1/s$) than that for $h_c +$ light hadrons ($\propto 1/s^2$), which clearly corroborates the dominance of the fragmentation mechanism at high energy (p_T).

V. PHENOMENOLOGY

With various color-singlet and color-octet short-distance coefficients determined in Secs. III and IV, we are ready to make a concrete analysis for the inclusive h_c production at B factories and assess its observation prospects.

A. Input parameters

At the B factory energy, we choose the running QED coupling constant $\alpha(\sqrt{s}) = 1/131$, and the running QCD coupling constant $\alpha_s(\sqrt{s}/2) \approx 0.211$. For the process $e^+e^- \rightarrow h_c +$ light hadrons, we take the occurring factorization scale $\mu = m_c$. An important source of the uncertainty in our predictions is rooted in the uncertainty about charm quark mass. We take the customary value $m_c = 1.5$ GeV, but allow it to float between 1.3 to 1.8 GeV in order to closely assess this uncertainty.

We need also specify the values of two nonperturbative NRQCD matrix elements appearing in the factorization formula (1). Upon vacuum saturation approximation, one can relate the color-singlet matrix element with the square of the first derivative of the radial wave function at the origin for $1P$ charmonium, which is calculable in quark potential models [14]:

$$\langle \mathcal{O}_1^{h_c}(^1P_1) \rangle \approx \frac{3}{2J+1} \langle \mathcal{O}_1^{\chi_{cJ}}(^3P_J) \rangle \approx \frac{9N_c}{2\pi} |R'_{1P}(0)|^2. \quad (28)$$

If the value of $R'_{1P}(0)$ is calculated from the Buchmüller-Tye potential model [34], one then finds $\langle \mathcal{O}_1^{h_c}(^1P_1) \rangle = 0.322 \text{ GeV}^5$.

In contrast to the color-singlet matrix element, no reliable phenomenological model calculations are available for the color-octet matrix element $\langle \mathcal{O}_8^{h_c}(^1S_0) \rangle$, since neither vacuum saturation approximation nor the quark potential models are applicable in this situation.

Fortunately, the approximate heavy quark spin symmetry in NRQCD can be invoked to connect the color-octet matrix elements of h_c and χ_{cJ} ($J = 0, 1, 2$) [14]:

$$\langle \mathcal{O}_8^{h_c}(^1S_0) \rangle \approx \frac{3}{2J+1} \langle \mathcal{O}_8^{\chi_{cJ}}(^3S_1) \rangle. \quad (29)$$

There have been available a number of phenomenological studies for inclusive χ_{cJ} production in hadron collision or in B decay experiments [8, 35–39], and the color-octet matrix elements $\langle \mathcal{O}_8^{\chi_{cJ}}(^3S_1) \rangle$ have been fitted by various groups over years. We can use (29) to translate their fitted color-octet matrix element for χ_{cJ} to the desired one for h_c . In Table I, we have enumerated some values of $\langle \mathcal{O}_8^{h_c}(^1S_0) \rangle$ excerpted from various references.

Alternatively, one can infer an order-of-magnitude estimate for the lower bound on $\langle \mathcal{O}_8^{h_c}(^1S_0) \rangle$ using the renormalization group equation (RGE), which governs the renormalization scale dependence of this color-octet matrix element. The solution to the RGE at leading order in α_s reads [14]

$$\langle \mathcal{O}_8^{h_c}(^1S_0) \rangle_{m_c} = \langle \mathcal{O}_8^{h_c}(^1S_0) \rangle_{\mu} + \frac{8C_F}{3N_c\beta_0} \ln \left(\frac{\alpha_s(\mu)}{\alpha_s(m_c)} \right) \frac{\langle \mathcal{O}_1^{h_c}(^1P_1) \rangle}{m_c^2}, \quad (30)$$

where $\beta_0 = \frac{11N_c - 2n_f}{3} = 9$ is the one-loop coefficient of QCD β function with $n_f = 3$ light quark flavors. The subscript of the color-octet matrix element specifies the renormalization

TABLE I: Variation of the predicted total cross sections for $e^+e^- \rightarrow h_c + \text{light hadrons}$ and for $e^+e^- \rightarrow h_c + \text{charmed hadrons}$ with the value of $\langle \mathcal{O}_8^{h_c}(^1S_0) \rangle$ (in units of GeV^3). We have taken $\alpha = 1/131$, $\alpha_s(\sqrt{s}/2) = 0.211$, $m_c = 1.5 \text{ GeV}$, and the color-singlet matrix element $\langle \mathcal{O}_1(^1P_1) \rangle = 0.322 \text{ GeV}^5$. The color-octet matrix element is taken from various references, while the last entry provides a lower bound inferred from the renormalization-group equation running in (31).

$\langle \mathcal{O}_8^{h_c}(^1S_0) \rangle$	Ref. [37, 38]	Ref. [39]	Ref. [8, 35]	Ref. [36]	RGE
Cross Section	0.009 – 0.01	0.022 – 0.025	0.014 – 0.020	0.039	≥ 0.0085
$e^+e^- \rightarrow h_c + X_{\text{LH}}$ (fb)	86.7 – 97.6	229.2 – 262.0	141.5 – 207.2	415.5	≥ 81.2
$e^+e^- \rightarrow h_c + X_{c\bar{c}}$ (fb)	9.9 – 10.0	10.2 – 10.3	10.1 – 10.2	10.7	≥ 9.9

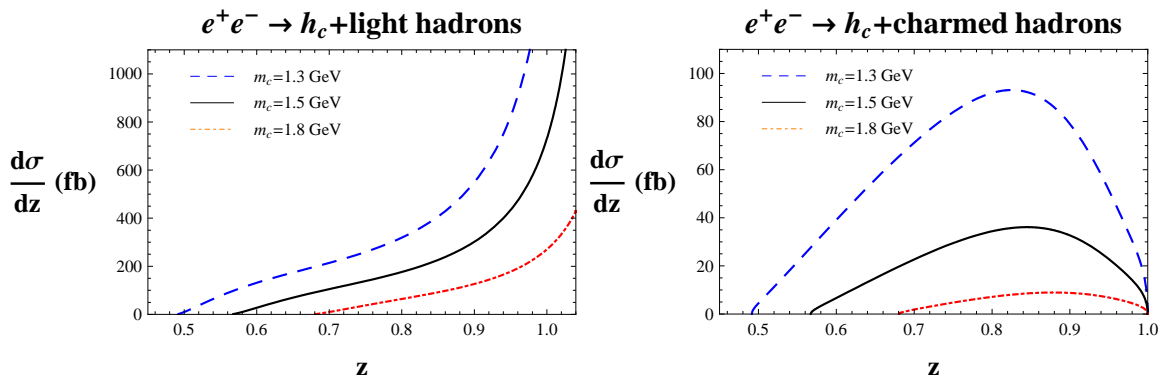


FIG. 1: The energy distribution of h_c in the processes $e^+e^- \rightarrow h_c + X_{\text{LH}}$ (left panel) and $e^+e^- \rightarrow h_c + X_{c\bar{c}}$ (right panel) at $\sqrt{s} = 10.58 \text{ GeV}$. The color-octet matrix element $\langle \mathcal{O}_8^{h_c}(^1S_0) \rangle$ is taken as 0.02 GeV^3 . Three curves in each plot correspond to taking $m_c = 1.3, 1.5, \text{ and } 1.8 \text{ GeV}$, respectively.

scale affiliated with the operator $\mathcal{O}_8^{h_c}(^1S_0)$. Taking $\mu = m_c v$, and assuming the matrix element $\langle \mathcal{O}_8^{h_c}(^1S_0) \rangle_{m_c v}$ is nonnegative, one then gets:

$$\langle \mathcal{O}_8(^1S_0) \rangle_{m_c} \geq \frac{32}{243} \ln \left(\frac{\alpha_s(m_c v)}{\alpha_s(m_c)} \right) \frac{\langle \mathcal{O}_1(^1P_1) \rangle}{m_c^2}. \quad (31)$$

Taking $\alpha_s(m_c) \sim 0.35$ and $\alpha_s(m_c v) \sim v \sim 0.55$, we then obtain $\langle \mathcal{O}_8(^1S_0) \rangle_{m_c} \gtrsim 0.0085 \text{ GeV}^3$. This estimate is of course a very rough one. Nevertheless, as one can clearly see from Table I, all the phenomenologically determined values for the matrix element $\langle \mathcal{O}_8^{h_c}(^1S_0) \rangle_{m_c}$ seem to be compatible with this bound.

In the following numerical analyses, we will take $\langle \mathcal{O}_8^{h_c}(^1S_0) \rangle_{m_c} = 0.02 \text{ GeV}^3$, a medium value among those tabulated in Table I.

B. Numerical results

Substituting the differential short-distance coefficients dF_n^{LH} ($n = 1, 8$) given in (4) and (17) into (1), we obtain the energy distribution of h_c in the process $e^+e^- \rightarrow h_c + \text{light hadrons}$ at B factory energy, as shown in the left panel of Fig. 1. Similarly, substituting the

differential coefficients dF_n^{Charm} ($n = 1, 8$) given in (22) and (23) into (1), we then obtain the energy spectrum of h_c in the process $e^+e^- \rightarrow h_c + \text{ charmed hadrons}$, as shown in the right panel of Fig. 1.

As can be clearly seen from Fig. 1, the h_c energy spectra in two production channels are markedly different. In the former case, the differential production rate of h_c sharply rises and diverges at the maximal energy of h_c ; while in the latter, the distribution turns over and vanishes as the energy of h_c approaches its maximum. As was discussed in Sec. III C, for the h_c production associated with light hadrons, our prediction to the high- z part of the h_c spectrum becomes untrustworthy, due to the breakdown of perturbative and velocity expansions near the endpoint region. An appropriate treatment requires resumming Sudakov logarithms as well as incorporating nonperturbative shape function, consequently one then expects the h_c spectrum will be smeared, and turn over near the upper endpoint, rather than diverge.

Our predictions for the integrated cross sections should be much more reliable than the differential distributions. Substituting the integrated short-distance coefficients F_n^{LH} ($n = 1, 8$), which are collected in (18), into (1), we obtain the total h_c production rate for the process $e^+e^- \rightarrow h_c + \text{ light hadrons}$; for the channel $e^+e^- \rightarrow h_c + \text{ charmed hadrons}$, the total cross section can be reached by numerically integrating the respective differential distribution.

With our default value for the color-octet matrix element $\langle \mathcal{O}_8^{h_c}(^1S_0) \rangle = 0.02 \text{ GeV}^3$, we estimate the total cross section for $h_c + \text{ light hadrons}$ to be about 207 fb, and that for $h_c + \text{ charmed hadrons}$ to be about 10 fb. In Table I, we have tabulated various predictions for the h_c total cross sections in both production channels by adopting different values of color-octet matrix elements, which are in the following range:

$$\sigma[e^+e^- \rightarrow h_c + X_{\text{LH}}] = 81.2 - 415.5 \text{ fb}, \quad (32a)$$

$$\sigma[e^+e^- \rightarrow h_c + X_{c\bar{c}}] = 9.9 - 10.7 \text{ fb}. \quad (32b)$$

One immediately observe that, the cross section of the former channel is quite sensitive to the value of $\langle \mathcal{O}_8^{h_c}(^1S_0) \rangle$, but that of the latter is not sensitive to it at all. This clearly indicates that the former process is dominated by the color-octet channel, while the latter is dominated by the color-singlet channel.

It is interesting to contrast the inclusive h_c production at B factories with the analogous inclusive J/ψ production processes, which have been recently measured by BELLE Collaboration [15]:

$$\sigma[e^+e^- \rightarrow J/\psi + X_{\text{LH}}] = 430 \pm 90 \pm 90 \text{ fb}, \quad (33a)$$

$$\sigma[e^+e^- \rightarrow J/\psi + X_{c\bar{c}}] = 740 \pm 80_{-80}^{+90} \text{ fb}. \quad (33b)$$

We see that the cross section for $h_c + \text{ light hadrons}$ is comparable in magnitude with the observed production rate for $J/\psi + \text{ light hadrons}$. In this work we have only implemented the color-octet short-distance coefficient F_8^{LH} at LO in α_s . It was recently discovered that there may exist a large positive $O(\alpha_s)$ correction to this coefficient [40]. If we include this perturbative correction, the total production rate for $h_c + \text{ light hadrons}$ may easily reach the value given in (33a). Therefore, copious $h_c + \text{ light hadrons}$ events should already have been produced at B factories.

In sharp contrast with inclusive J/ψ production, our predicted production rate for $h_c + \text{ charmed hadrons}$ are about one order of magnitude smaller than that for $h_c + \text{ light hadrons}$.

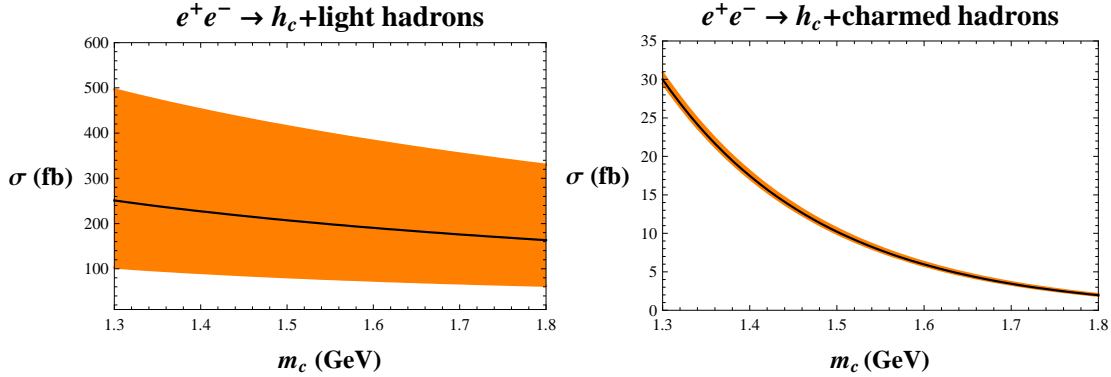


FIG. 2: The total production rate for h_c as a function of m_c at $\sqrt{s} = 10.58$ GeV. The left panel is for the process $e^+e^- \rightarrow h_c + X_{\text{LH}}$, and the right panel is for $e^+e^- \rightarrow h_c + X_{c\bar{c}}$. The band in each plot characterizes the uncertainty estimated by varying the color-octet matrix element $\langle \mathcal{O}_8^{h_c}(^1S_0) \rangle$ from 0.0085 to 0.039 GeV^3 , where the central curve corresponds to fixing $\langle \mathcal{O}_8^{h_c}(^1S_0) \rangle$ at 0.02 GeV^3 .

This is a normal hierarchy pattern, being consistent with the heuristic expectation based on the kinematics consideration. Practically speaking, the low production rate may render the experimental measurements of this production channel of h_c difficult.

One should caution that, the predicted h_c production rates given in (32) are still subject to large theoretical uncertainty. Besides the value of $\langle \mathcal{O}_8^{h_c}(^1S_0) \rangle$, the charm quark mass constitutes one major source of the uncertainty. In Fig. 2 we explicitly show how the total production rates for h_c vary with m_c . A useful message conveyed by Fig. 2 is that, the production rate for $e^+e^- \rightarrow h_c + \text{charmed hadrons}$ is much more sensitive to m_c than that for $e^+e^- \rightarrow h_c + \text{light hadrons}$ (this point can also be seen in Fig. 1). This fact can be best explained by going to the asymptotic limit $\sqrt{s} \gg m_c$. In such a limit, the process $e^+e^- \rightarrow h_c + X_{c\bar{c}}$ is dominated by the color-singlet fragmentation mechanism, thus in light of (27), one expects $\sigma \propto \langle \mathcal{O}_1^{h_c}(^1P_1) \rangle / m_c^5$. The process $e^+e^- \rightarrow h_c + X_{\text{LH}}$ is dominated by the color-octet channel, from (19b), one finds that asymptotically, $\sigma \propto \langle \mathcal{O}_8(^1S_1) \rangle / m_c$. It is this very different power-law scaling behavior that accounts for the much stronger sensitivity of $\sigma[e^+e^- \rightarrow h_c + X_{c\bar{c}}]$ to charm quark mass.

Finally, in Fig. 3 we show how the integrated h_c production rates vary with the center-of-mass energy. As can be clearly seen, as \sqrt{s} increases, the total cross section of $e^+e^- \rightarrow h_c + X_{\text{LH}}$ descends much steeper than that of $e^+e^- \rightarrow h_c + X_{c\bar{c}}$. This can be easily attributed to the fact that at large s , the production rate in the former process scales as $1/s^2$, while that in the latter case scales only as $1/s$, as dictated by the fragmentation mechanism.

C. Observation prospects of inclusive h_c production at B factories

Thus far, there is yet no any experiment at B factories dedicated to measure the inclusive h_c production rate. Perhaps it is partly due to the lack of phenomenological incentive, and more importantly, due to the difficulty of reconstructing the h_c signals.

Our prediction in (32), indicates that a large number of $h_c + \text{light hadrons}$ events should have already been produced at B factories, given the large integrated luminosity that has

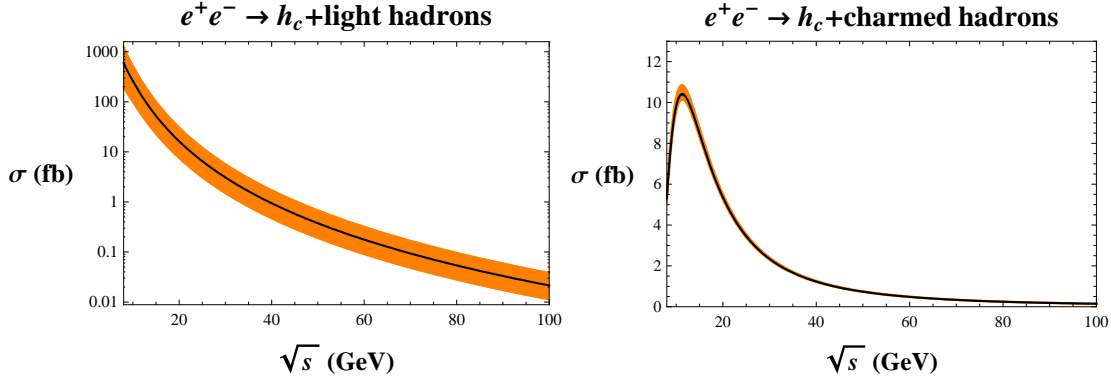


FIG. 3: The integrated h_c production cross section as a function of \sqrt{s} for the processes $e^+e^- \rightarrow h_c + X_{\text{LH}}$ (left panel) and $e^+e^- \rightarrow h_c + X_{c\bar{c}}$ (right panel). The band in each plot measures the uncertainty brought in by varying the color-octet matrix element $\langle \mathcal{O}_8^{h_c}(^1S_0) \rangle$ from 0.0085 to 0.039 GeV^3 , where the central curve corresponds to fixing $\langle \mathcal{O}_8^{h_c}(^1S_0) \rangle$ at 0.02 GeV^3 .

been accumulated by two B factory experiments near the $\Upsilon(4S)$ resonance. As we have shown before, the prospective measurements of this channel would provide a unique opportunity to test the color-octet mechanism in quarkonium production, and impose useful constraint on the color-octet matrix element $\langle \mathcal{O}_8^{h_c}(^1S_0) \rangle$. In view of this, there should be sufficient phenomenological impetus for experimentalists to pursue this measurement.

We can examine the observation potential for inclusive h_c production more quantitatively. Up to present, BELLE experiment has accumulated about 1000 fb^{-1} data near the $\Upsilon(4S)$ resonance. Taking $\sigma[e^+e^- \rightarrow h_c + X_{\text{LH}}] \approx 100 - 400 \text{ fb}$ from (32a), we thus estimate that roughly $(1 - 4) \times 10^5$ h_c events have been produced at BELLE at $\sqrt{s} = 10.58 \text{ GeV}$.

The two major decay channels of h_c so far observed are $h_c \rightarrow 2(\pi^+\pi^-)\pi^0$ and $h_c \rightarrow \eta_c\gamma$, with comparable branching fractions. The η_c hadronic decay is probably not a good tagging mode for h_c due to the appearance of π^0 in the final state. Rather it seems superior to use the $E1$ transition $h_c \rightarrow \eta_c\gamma$ to reconstruct the h_c signal, i.e., first reconstruct an η_c , then check if there exists a narrow peak around 3525 MeV in $\gamma + \eta_c$ invariant mass distribution.

The main experimental difficulty hinges on how to efficiently reconstruct the η_c . Recently, BELLE Collaboration has searched for the radiative decay processes $\Upsilon(1S, 2S) \rightarrow \gamma\eta_c$ [41, 42], and developed some method to effectively tag η_c . They reconstruct the η_c meson via several hadronic decay modes, *e.g.* $K_S K^+ \pi^- + c.c.$, $\pi^+ \pi^- K^+ K^-$, $2(K^+ K^-)$, $2(\pi^+ \pi^-)$, $3(\pi^+ \pi^-)$ by looking for the charged tracks. A conservative estimate gives that about 1% η_c events can be reconstructed⁵.

Taking $\mathcal{B}(h_c \rightarrow \gamma\eta_c) \approx 50\%$ [5], we then expect roughly $(1 - 4) \times 10^5 \times 50\% \times 1\% = 500 - 2000$ reconstructed h_c events.

A large number of reconstructed h_c events seems to indicate a bright observation prospect, however, one must be alert to the potentially huge combinatorial background, since there

⁵ This estimate is obtained from the product of detection efficiency and the branching fractions of aforementioned η_c decay channels. With the efficiency taken with around 25%, it is reasonable to assume that 1% η_c events will be reconstructed. We thank C. Z. Yuan for providing this estimate and for explaining to us some experimental details.

are a lot of pions, kaons and photons in the events. A careful study of the background level is crucial from the experimental perspective.

VI. SUMMARY

In this work, we have studied the inclusive production of the h_c meson associated with light hadrons and with charmed hadrons at B factories, respectively, in the framework of NRQCD factorization. We have only considered the lowest-order contribution in v , which involves both the color-singlet $^1P_1^{(1)}$ channel and the color-octet $^1S_0^{(8)}$ channel.

We have explicitly verified that, for $e^+e^- \rightarrow h_c +$ light hadrons, including the color-octet channel is pivotal in rendering infrared-finite prediction for the inclusive h_c production rate. Moreover, at B factory energy $\sqrt{s} = 10.58$ GeV, within some reasonable choices for the color-octet matrix element $\langle \mathcal{O}_8^{h_c}(^1S_0) \rangle$, we find that the total h_c production rate varies in the range between 0.08 and 0.4 pb. Furthermore, this process is found to be dominated by the color-octet channel. Future measurement of this process at B factories may provide an explicit test on the color-octet mechanism, as well as put useful constraint on the value of the color-octet matrix element $\langle \mathcal{O}_8^{h_c}(^1S_0) \rangle$.

For the process $e^+e^- \rightarrow h_c +$ charmed hadrons, we find that the total production rate is almost saturated by the color-singlet channel. The predicted total production cross section at $\sqrt{s} = 10.58$ GeV is about 10 fb if taking the charm quark mass to be 1.5 GeV. This is about one order-of-magnitude smaller than the cross section for $e^+e^- \rightarrow h_c +$ light hadrons. We note that this prediction bears large uncertainty, for it is quite sensitive to the charm quark mass. If allowing m_c to float from 1.8 GeV to 1.3 GeV, this cross section would vary from a few fb to 30 fb. It is interesting to see if the future experiments can observe this process.

Acknowledgments

We thank Chang-Zheng Yuan for helpful discussions. This research was supported in part by the National Natural Science Foundation of China under Grant No. 10875130, No. 10935012, and by China Postdoctoral Science Foundation.

Appendix A: Isolating the infrared divergence for $e^+e^- \rightarrow c\bar{c}(^1P_1^{(1)}) + gg$ in dimensional regularization

In this Appendix, we explain how to calculate the IR-divergent integral in (12a) in dimensional regularization. The D -dimensional 3-body phase space measure $d\Phi_3$ and the integrand $I_{\text{div}}(x_1, z)$ have already been presented in (6) and (10), respectively. Inspecting these expressions, one can readily recognize that the IR singularity would arise from two distinct phase space corners: $z \rightarrow 1 + r, x_1 \rightarrow 0$ and $z \rightarrow 1 + r, x_1 \rightarrow 1 - r (x_2 \rightarrow 0)$, by integrating the first and second terms in (10), respectively.

First note that both the integrand and the phase space measure in (12a) are symmetric under the interchange $x_1 \leftrightarrow x_2$. A useful shortcut to perform the x_1 -integral is to integrate

over only the lower half of its allowed range, then multiply the result by 2:

$$\int_{a(z)-b(z)}^{a(z)+b(z)} dx_1 = 2 \int_{a(z)-b(z)}^{a(z)} dx_1, \quad (\text{A1})$$

where $a(z)$ and $b(z)$ are defined in (8). As a simplification, the IR singularity now is solely caused by the first term in (10), when integrated over the phase space corner $z \rightarrow 1+r, x_1 \rightarrow 0$. The integral involving the second term now becomes IR finite, thereby can be worked out directly in 4 dimensions.

We then face the IR-divergent integral of the following type:

$$I(z) = \int_{a(z)-b(z)}^{a(z)} dx_1 \frac{g(x_1, z)}{(1+r-z-x_1)^2 x_1^{2\epsilon} (1-\cos^2\theta)^\epsilon}, \quad (\text{A2})$$

where $\cos\theta$ as a function of z and x_1 has been given in (7), and $g(x_1, z)$ is an arbitrary function that is regular at $z = 1+r$. Note that the ϵ -dependent factors in the integrand come from the D -dimensional 3-body phase space measure, playing the role of the IR regulator.

A brute-force calculation of $I(z)$ while keeping the full ϵ dependence is a challenging task, if not impossible. It is desirable if one can make the IR divergence explicit prior to carrying out the x_1 integration. This is indeed feasible, and in the analysis of the decay process $\chi_{bJ} \rightarrow c\bar{c}g$, Bodwin *et al.* [25] have elaborated on how to fulfill such a goal by utilizing a simple trick. In below, we will employ a strategy that is closely analogous to theirs⁶.

The key is to realize that $x_1^+ x_1^- = a^2(z) - b^2(z) = 1+r-z$. As suggested by this identity, it may seem advantageous to introduce a new integration variable t :

$$t = \frac{1+r-z}{x_1} = a(z) + b(z) \cos\theta. \quad (\text{A3})$$

The integration range for this new variable turns out to be $t_0 \leq t \leq a(z) + b(z)$, where

$$t_0 = \frac{2(1+r-z)}{2-z}. \quad (\text{A4})$$

In term of the new variable t , equation (A2) becomes

$$I(z) = \frac{1}{(1+r-z)^{1+2\epsilon}} \int_{t_0}^{a(z)+b(z)} dt \frac{t^{2\epsilon}}{(1-t)^2} \frac{g(t, z)}{(1-\cos^2\theta)^\epsilon}. \quad (\text{A5})$$

In light of (A3), $\cos\theta$ now should be understood as a function of t , $a(z)$ and $b(z)$.

With the aid of the familiar identity about distributions, we can express $(1+r-z)^{-1-2\epsilon}$ as

$$\frac{1}{(1+r-z)^{1+2\epsilon}} = -\frac{\delta(1+r-z)}{2\epsilon(1-\sqrt{r})^{4\epsilon}} + \left[\frac{1}{1+r-z} \right]_+ - 2\epsilon \left[\frac{\ln(1+r-z)}{1+r-z} \right]_+ \dots \quad (\text{A6})$$

⁶ We note that the process $\eta_b \rightarrow \chi_{cJ} + gg$ ($J = 0, 1, 2$) has recently been analyzed in NRQCD factorization [43], which shares essentially the identical kinematics as our process. The methodology of isolating the IR singularity in DR in [43] is similar to what is adopted in [25].

As advertised, we have successfully separated the IR pole that is accompanied with the $\delta(1+r-z)$ function. The IR-regular remainders are partially encoded in the “+”-functions, whose integration property has been specified in (14). To the desired accuracy, the logarithmic “+” function is not needed in this work.

One can be readily convinced that the integral in (A5) is finite in the limit $\epsilon \rightarrow 0$. Therefore, to our intended accuracy, it can be evaluated by simply Taylor-expanding the integrand through the first order in ϵ .

Using the master formulas (A5) and (A6), it is now a straightforward exercise to reproduce the analytic expression of $d\hat{\sigma}_{\text{div}}/dz$ as given in (13a). One can further integrate this expression over z to arrive at

$$\hat{\sigma}_{\text{div}} = \frac{128\pi e_c^2 \alpha^2 C_F \alpha_s^2 (1-r)}{3m_c^2 s} \frac{c_\epsilon (4\pi)^\epsilon}{\Gamma(1-\epsilon)} \left[-\frac{1}{\epsilon_{\text{IR}}} - 2 \ln \frac{\mu^2}{4m_c^2} + 4 \ln(1-r) - \frac{1-3r}{1-r} \ln r - 1 \right]. \quad (\text{A7})$$

Appendix B: η_c production associated with charmed hadrons in e^+e^- annihilation

In this Appendix, we consider $e^+e^- \rightarrow \eta_c +$ charmed hadrons at lowest order in v and α_s (note that $e^+e^- \rightarrow \eta_c + gg$ is forbidden by the charge conjugation invariance). The result presented in this section can be viewed as a byproduct of the analysis made in Sec. IV. We note that, the process $e^+e^- \rightarrow \eta_c + c\bar{c}$ has already been investigated some time ago [32], and our calculation may serve as an independent check.

At the lowest order in v , the NRQCD factorization formula for the η_c inclusive production reads [14]:

$$d\sigma[e^+e^- \rightarrow \eta_c + X_{c\bar{c}}] = \frac{dF_1^{\text{Charm}}}{m_c^2} \langle \mathcal{O}_1^{\eta_c}(^1S_0) \rangle + O(\sigma v^2), \quad (\text{B1})$$

where the color-singlet production operator $\mathcal{O}_1^{\eta_c}(^1S_0)$ has been defined in [14], dF_1^{Charm} is the corresponding short-distance coefficient. Unlike the P -wave charmonium production, here we are justified to ignore the color-octet channel since its relative importance is suppressed by v^4 .

The perturbative matching calculation for the color-singlet short-distance coefficient is

completely analogous to Sec. IV, and we directly present the result:

$$\begin{aligned}
\frac{dF_1^{\text{Charm}}}{dz} = & \frac{32\pi e_c^2 \alpha_s^2}{81m_c s(2-z)^2 z^3} \left\{ \frac{2z}{3(2-z)^4} \sqrt{\frac{(1-z)(z^2-4r)}{1+r-z}} \times \right. \\
& \left[96r^3(1+r) - 96r^2(4+6r+r^2)z + 16(6-25r+38r^2+43r^3-2r^4)z^2 \right. \\
& - 8(24-138r+58r^2+51r^3-r^4)z^3 + (112-944r+372r^2+118r^3-6r^4)z^4 \\
& \left. - 2(24-120r+62r^2+r^3)z^5 + (54+5r+13r^2)z^6 - (28+11r)z^7 + 6z^8 \right] \\
& + r \ln \left(\frac{z\sqrt{1+r-z} + \sqrt{(1-z)(z^2-4r)}}{z\sqrt{1+r-z} - \sqrt{(1-z)(z^2-4r)}} \right) \left[8r^3 - 32r^2z - 2(4-6r-r^3)z^2 \right. \\
& \left. \left. - 4r(1+r)z^3 + (10+r)z^4 \right] \right\}. \tag{B2}
\end{aligned}$$

Our expression seems to be considerably compact than its counterpart in [32]. We have numerically checked that once using their phenomenological input parameters, we can reproduce their predicted production rate for $\eta_c + X_{c\bar{c}}$ at B factory energy.

Similar to the fragmentation function of c into h_c in (25), the fragmentation function of c into η_c can also be factorized as

$$D_{c \rightarrow \eta_c}(z) = d_1^{\eta_c}(z) \frac{\langle \mathcal{O}_1^{\eta_c}(^1S_0) \rangle}{m_c^3} + O(v^2), \tag{B3}$$

where $d_1^{\eta_c}(z)$ is the color-singlet coefficient function, which agrees with the one give in [?].

Following the steps described in Sec. IV C, it is straightforward to identify $d_1^{\eta_c}(z)$ by taking the asymptotic limit to (B2):

$$d_1^{\eta_c}(z) = \left. \frac{m_c}{2\tilde{\sigma}} \frac{dF_1^{\text{Charm}}}{dz} \right|_{\text{asym}} = \frac{16\alpha_s^2 z(1-z)^2 (48 + 8z^2 - 8z^3 + 3z^4)}{243(2-z)^6}, \tag{B4}$$

which fully agrees exactly with the fragmentation function of $c \rightarrow \eta_c$ first obtained in [? ?]. Obviously, this expression only differs with $d_g^{h_c}$ in (26) by a color factor.

Finally we assess the integrated cross section for $e^+e^- \rightarrow \eta_c + X_{c\bar{c}}$. It is difficult to obtain the analytic result by integrating (B2) over z . Nevertheless we are content with knowing its asymptotic behavior by resorting to fragmentation approximation:

$$\begin{aligned}
\sigma[e^+e^- \rightarrow \eta_c + X_{c\bar{c}}] \Big|_{\text{asym}} &= 2\tilde{\sigma} \int_0^1 dz D_{c \rightarrow \eta_c}(z) \\
&= 16\alpha_s^2 \tilde{\sigma} \frac{773 - 1110 \ln 2}{1215} \frac{\langle \mathcal{O}_1^{\eta_c}(^1S_0) \rangle}{m_c^3}. \tag{B5}
\end{aligned}$$

This expression is compatible with the one give in [?].

[1] J. L. Rosner *et al.* [CLEO Collaboration], Phys. Rev. Lett. **95**, 102003 (2005) [hep-ex/0505073]; P. Rubin *et al.* [CLEO Collaboration], Phys. Rev. D **72**, 092004 (2005) [hep-ex/0508037].

- [2] M. Andreotti *et al.* [E835 Collaboration], A. Buzzo, R. Calabrese and R. Cester *et al.*, Phys. Rev. D **72**, 032001 (2005).
- [3] I. Adachi *et al.* [Belle Collaboration], Phys. Rev. Lett. **108**, 032001 (2012) [arXiv:1103.3419 [hep-ex]].
- [4] S. Dobbs *et al.* [CLEO Collaboration], Phys. Rev. Lett. **101**, 182003 (2008) [arXiv:0805.4599 [hep-ex]].
- [5] M. Ablikim *et al.* [BESIII Collaboration], Phys. Rev. Lett. **104**, 132002 (2010) [arXiv:1002.0501 [hep-ex]].
- [6] G. S. Adams *et al.* [CLEO Collaboration], Phys. Rev. D **80**, 051106 (2009) [arXiv:0906.4470 [hep-ex]].
- [7] T. K. Pedlar *et al.* [CLEO Collaboration], Phys. Rev. Lett. **107**, 041803 (2011) [arXiv:1104.2025 [hep-ex]].
- [8] M. Beneke, F. Maltoni and I. Z. Rothstein, Phys. Rev. D **59**, 054003 (1999) [arXiv:hep-ph/9808360];
- [9] G. T. Bodwin, E. Braaten, T. C. Yuan and G. P. Lepage, Phys. Rev. D **46**, 3703 (1992) [hep-ph/9208254].
- [10] S. Fleming and T. Mehen, Phys. Rev. D **58**, 037503 (1998) [hep-ph/9801328].
- [11] K. Sridhar, Phys. Lett. B **674**, 36 (2009) [arXiv:0812.0474 [hep-ph]].
- [12] C. -F. Qiao, D. -L. Ren and P. Sun, Phys. Lett. B **680**, 159 (2009) [arXiv:0904.0726 [hep-ph]].
- [13] For a recent review on quarkonium production and various aspects of quarkonium physics, see N. Brambilla *et al.*, Eur. Phys. J. C **71**, 1534 (2011).
- [14] G. T. Bodwin, E. Braaten and G. P. Lepage, Phys. Rev. D **51**, 1125 (1995) [Erratum-ibid. D **55**, 5853 (1997)].
- [15] P. Pakhlov *et al.* [Belle Collaboration], Phys. Rev. D **79**, 071101 (2009) [arXiv:0901.2775 [hep-ex]].
- [16] J. Xu, Ph.D. thesis, *Electromagnetic transitions of quarkonia and productions of P-wave quarkonia*, IHEP (2011) (in Chinese).
- [17] W. Y. Keung, Phys. Rev. D **23**, 2072 (1981).
- [18] A. Petrelli, M. Cacciari, M. Greco, F. Maltoni and M. L. Mangano, Nucl. Phys. B **514**, 245 (1998) [arXiv:hep-ph/9707223].
- [19] G. 't Hooft and M. J. G. Veltman, Nucl. Phys. B **44**, 189 (1972);
P. Breitenlohner and D. Maison, Commun. Math. Phys. **52**, 11 (1977).
- [20] T. H. West, Comput. Phys. Commun. **77**, 286 (1993).
- [21] G. C. Nayak, J. W. Qiu and G. Sterman, Phys. Lett. B **613**, 45 (2005) [arXiv:hep-ph/0501235].
- [22] G. C. Nayak, J. W. Qiu and G. Sterman, Phys. Rev. D **72**, 114012 (2005) [arXiv:hep-ph/0509021].
- [23] G. C. Nayak, J. W. Qiu and G. Sterman, Phys. Rev. D **74**, 074007 (2006) [arXiv:hep-ph/0608066].
- [24] J. P. Ma and Z. G. Si, Phys. Lett. B **625**, 67 (2005) [hep-ph/0506078].
- [25] G. T. Bodwin, E. Braaten, D. Kang and J. Lee, Phys. Rev. D **76**, 054001 (2007) [arXiv:0704.2599 [hep-ph]].
- [26] M. Beneke, I. Z. Rothstein, and M. B. Wise, Phys. Lett. B **408**, 373 (1997) [arXiv:hep-ph/9705286].
- [27] M. Beneke, G. A. Schuler and S. Wolf, Phys. Rev. D **62**, 034004 (2000) [arXiv:hep-ph/0001062].
- [28] S. Fleming, A. K. Leibovich and T. Mehen, Phys. Rev. D **68**, 094011 (2003) [arXiv:hep-

- ph/0306139].
- [29] Y. Jia, Phys. Rev. D **82**, 034017 (2010) [arXiv:0912.5498 [hep-ph]].
 - [30] Z. -B. Kang, J. -W. Qiu and G. Sterman, Phys. Rev. Lett. **108**, 102002 (2012) [arXiv:1109.1520 [hep-ph]].
 - [31] P. L. Cho and A. K. Leibovich, Phys. Rev. D **54**, 6690 (1996) [arXiv:hep-ph/9606229].
 - [32] K. -Y. Liu, Z. -G. He and K. -T. Chao, Phys. Rev. D **69**, 094027 (2004) [hep-ph/0301218].
 - [33] T. C. Yuan, Phys. Rev. D **50**, 5664 (1994) [hep-ph/9405348].
 - [34] E. J. Eichten and C. Quigg, Phys. Rev. D **52**, 1726 (1995) [hep-ph/9503356].
 - [35] B. Gong, L. -P. Wan, J. -X. Wang and H. -F. Zhang, arXiv:1205.6682 [hep-ph].
 - [36] Y. -Q. Ma, K. Wang and K. -T. Chao, Phys. Rev. D **83**, 111503 (2011) [arXiv:1002.3987 [hep-ph]].
 - [37] E. Braaten and S. Fleming, Phys. Rev. Lett. **74**, 3327 (1995) [hep-ph/9411365];
 - [38] P. L. Cho and A. K. Leibovich, Phys. Rev. D **53**, 6203 (1996) [hep-ph/9511315].
 - [39] M. Cacciari, M. Greco, M. L. Mangano and A. Petrelli, Phys. Lett. B **356**, 553 (1995) [hep-ph/9505379]; E. Braaten, S. Fleming and T. C. Yuan, Ann. Rev. Nucl. Part. Sci. **46**, 197 (1996) [hep-ph/9602374].
 - [40] Y. -J. Zhang, Y. -Q. Ma, K. Wang and K. -T. Chao, Phys. Rev. D **81**, 034015 (2010) [arXiv:0911.2166 [hep-ph]].
 - [41] C. P. Shen *et al.* [Belle Collaboration], Phys. Rev. D **82**, 051504 (2010) [arXiv:1008.1774 [hep-ex]].
 - [42] X. L. Wang *et al.* [Belle Collaboration], Phys. Rev. D **84**, 071107 (2011) [arXiv:1108.4514 [hep-ex]].
 - [43] Z. -G. He and B. -Q. Li, Phys. Lett. B **693**, 36 (2010) [arXiv:0910.0220 [hep-ph]].